

# Two-Pass Rate Control for Improved Quality of Experience in UHDTV Delivery

Ivan Zupancic, *Student Member, IEEE*, Matteo Naccari, *Member, IEEE*, Marta Mrak, *Senior Member, IEEE*, and Ebroul Izquierdo, *Senior Member, IEEE*

**Abstract**—Rate control plays an important role in any video coding application and it was extensively studied in the context of previous video coding standards. However, the current state-of-the-art high efficiency video coding (HEVC) standard introduces many flexible tools making previous rate-distortion models used in rate control insufficiently accurate. Recently, a few rate control methods have been developed for HEVC that introduce many useful features, such as a robust correspondence between the rate and Lagrange multiplier  $\lambda$ . Nonetheless, previous rate control algorithms for HEVC do not address typical content in television applications that consists of frequent scene changes. Furthermore, the new ultra high definition television (UHDTV) format, which is expected to become widespread in the future, demands for even higher compression efficiency. To overcome these issues, a two-pass rate control method is proposed in this paper, targeting the encoding of UHDTV content. In the first pass, a fast encoder with limited set of coding tools is used during pre-encoding step to obtain the data used for rate allocation and model parameter initialization, which will then be used during the second pass. To avoid multiple encoding steps when deriving this information, a variable quantization parameter framework is proposed. Experimental results show that the proposed rate control method outperforms the well-known HEVC rate control method. When compared with variable bit-rate encoding mode, the proposed two-pass rate control method achieves on average 2.9% BD-rate losses. That is significantly better than the state-of-the-art HEVC rate control method, which achieves an average 8.8% BD-rate loss. The proposed method also provides a more consistent quality fluctuation with time, measured with standard deviation of frame PSNR values, required for high Quality of Experience.

**Index Terms**—HEVC, quality of experience, rate control, UHD video, video streaming.

## I. INTRODUCTION

ULTRA high definition television (UHDTV) is the new format which is expected to deliver a greater impact, more presence and immersion than the current high definition television (HDTV). UHDTV is not just about more pixels but it has the potential to deliver wider color gamut, high dynamic

Manuscript received March 7, 2016; revised September 2, 2016; accepted November 14, 2016. Date of publication; date of current version. Part of the work described in this paper has been conducted within the project COGNITUS. This work was supported by the European Union's Horizon 2020 research and innovation programme under Grant 687605. The guest editor coordinating the review of this paper and approving it for publication was Prof. Alexander Raake.

I. Zupancic and E. Izquierdo are with the School of Electronic Engineering and Computer Science, Queen Mary University of London, London E1 4NS, U.K. (e-mail: i.zupancic@qmul.ac.uk; ebroul.izquierdo@qmul.ac.uk).

M. Naccari and M. Mrak are with the British Broadcasting Corporation, London W12 7SB, U.K. (e-mail: matteo.naccari@bbc.co.uk; marta.mrak@bbc.co.uk).

Digital Object Identifier 10.1109/JSTSP.2016.2634458

range and high frame rate; in other words, it will ultimately provide users with *better* pixels. The parameters for UHDTV are specified in the ITU Recommendation BT.2020 [1] where two spatial resolutions are standardized:  $3840 \times 2160$  luma samples/frame and  $7680 \times 4320$  luma samples/frame, both of which are integer multiples of the  $1920 \times 1080$  (HDTV) picture size. Temporal resolutions for UHDTV can go up to 120 frames per second (fps) with progressive scanning only. It also allows 10- and 12-bit color depth, while the colorimetry system is wider than the one specified in Recommendation ITU-R BT.709 [2] for HDTV content, and covers 75.8% of the CIE 1931 color space. The chrominance sampling ratios included in BT.2020 are 4:2:0, 4:2:2 and 4:4:4.

Based on BT.2020, which defines the parameters of UHDTV services from the signal perspective, other organizations such as Digital Video Broadcasting (DVB) and European Broadcasting Union (EBU) have been working towards the definition of the parameters needed by applications which make use of UHDTV content. DVB has recently ratified the parameters for the delivery of UHDTV (“UHD-1 phase 1”) services (they are published as version 2.1.1 of ETSI TS 101 154 [3]): spatial resolution of  $3840 \times 2160$ , maximum bit-depth of 10 bits, temporal resolution up to 60 fps, and BT.709 colorimetry.

Even with the simplest form of UHDTV content, which only increases the number of pixels compared to HDTV, the volume of data associated with UHDTV content is at least four times that for HDTV content. Therefore, in order to reduce the UHDTV burden on the distribution networks, improved compression techniques should be employed when delivering UHDTV services. As an answer to these needs, the ITU-T Video Coding Experts Group (VCEG) and the ISO/IEC Moving Picture Experts Group (MPEG) have finalized the Version 1 of H.265/high efficiency video coding (HEVC) standard [4] in January 2013. HEVC is the state-of-the-art in video compression and can provide the same perceived video quality as its predecessor H.264/advanced video coding (AVC) [5] at half of the bit-rate [6]. For UHDTV content, the MPEG final verification tests have shown an average bit-rate reduction of up to 60% [7].

Even though improved compression technology is key in enabling the delivery of UHDTV content, it is also equally important to distribute the available bit-budget so that the impact of video coding artifacts is minimized. This is particularly true for UHDTV services given the high expectations of audiences. This paper considers as its application scenario the delivery of nearly live UHDTV video over streaming platforms, such as BBC iPlayer, using the HEVC standard. Accordingly, a given

90 amount of latency (e.g. few seconds) in the playout is tolerated  
 91 as well as some bit-rate fluctuations around the target value  
 92 with time (e.g. up to 30% above the target rate within a pe-  
 93 riod of 3 seconds). This application scenario can be extended  
 94 to any practical video coding application under constant bit-rate  
 95 (CBR) constraints. A major requirement is that coding artifacts  
 96 such as blocking, blurring, and contouring should be minimized.  
 97 Moreover, the video quality should stay constant over the time,  
 98 especially when an intra coded frame is inserted because of a  
 99 scene change.

100 Rate control guarantees that the available bit-budget is dis-  
 101 tributed so that the video quality is maximized. A rate control  
 102 method aims to optimize the visual quality given the limited  
 103 bandwidth constraints. Generally speaking, rate control can be  
 104 divided into two main steps. The first one allocates the right  
 105 amount of bits to each level of the coding process, i.e. structure  
 106 of pictures (SOP), frame, macroblock or coding unit (CU) in  
 107 HEVC. In the second step, the allocated rate is used to derive  
 108 the amount of compression to be applied over a given part of  
 109 the video sequence.

110 Rate control can be performed in single- or multi-pass fash-  
 111 ion. Single-pass rate control methods allocate the available rate  
 112 and tune the encoding based on some *a priori* knowledge on the  
 113 sequence statistics or data collected over previously encoded  
 114 frames. Contrarily, multi-pass controllers encode a given video  
 115 segment multiple times, where the results of one step are then  
 116 used in the subsequent ones. Single-pass rate control is usually  
 117 employed in applications with real time or very low latency re-  
 118 quirements, such as live broadcasting or production. Conversely,  
 119 multi-pass rate control is usually employed in near real-time ap-  
 120 plications with continuous scene changes, such as on-demand  
 121 services, where additional computational complexity can be tol-  
 122 erated.

123 This paper proposes a two-pass rate control method for  
 124 streaming of UHD TV content using Version 1 of the HEVC  
 125 standard. In the first pass, the algorithm performs a pre-encoding  
 126 analysis, where a light complexity encoder is used to compress  
 127 the number of frames associated with one intra period, and  
 128 then collect information such as bit-rate distribution over dif-  
 129 ferent frames. This information is then used to fit and update  
 130 the models used to decide the quantization steps to be used over  
 131 different frames and image areas, while performing the actual  
 132 compression in the second pass. The proposed method achieves  
 133 improved performance compared to existing approaches, espe-  
 134 cially at the beginning of each scene. The latency introduced by  
 135 the proposed rate control method is minimal and mainly asso-  
 136 ciated with the pre-processing stage. The proposed rate control  
 137 method does not imply any additional constraint on the size of  
 138 the coded picture buffer (CPB). In fact, once the pre-analysis  
 139 stage is concluded, the actual encoding can start and bit allo-  
 140 cation can be adjusted (e.g. on a frame basis) to meet the CPB  
 141 size constraints specified by HEVC for a particular level and  
 142 tier. Overall, the main contributions brought by the paper can be  
 143 summarized as follows:

144 1) Use of a low complexity pre-encoding step which pro-  
 145 vides an accurate estimate of the bit-rate profile spent on  
 146 different frames.

- 2) Content adaptive initialization of parameters for the rate-  
 quantization step model, based on the data collected dur-  
 ing the pre-encoding step.
- 3) Automatic derivation of initial quantization step for each  
 sequence based on a simplified encoding method which  
 uses multiple quantization steps within a frame.

The remainder of this paper is organized as follows. An  
 overview of the existing rate control methods with the emphasis  
 on the state-of-the-art methods designed for HEVC is presented  
 in Section II. The proposed two-pass rate control method is  
 described in detail in Section III, while Section IV presents a  
 comprehensive experimental validation of the proposed algo-  
 rithm. Finally, Section V concludes the paper and points out  
 some future work related to the proposed method.

## II. OVERVIEW OF THE RELATED BACKGROUND

As stated in the Introduction, rate control is one of the essen-  
 tial tools for any practical video codec and consists of two main  
 steps: rate allocation at different granularity levels (e.g. SOP,  
 frame, and block level) and derivation of coding parameters for  
 a given target rate. Over the years, literature has mainly focused  
 on the second step by proposing different models to express the  
 relationship between coding rate and parameters.

This section provides an overview of the existing rate control  
 methods and is organized into four subsections where the first  
 three review the literature associated with models for coding  
 parameters derivation, multi-pass algorithms, and algorithms  
 devoted to improve the perceived video quality. Finally, the  
 fourth subsection focuses on the efficient method based on  
 $R - \lambda$  model, which serves as a basis for our novel two-pass  
 rate control method.

### A. Modeling the Coding Rate and Parameters Relationship

One of the first attempts to model the relationship between  
 coding rate and quantization parameter (QP) dates back to the  
 MPEG-2 Video standard with the rate control method imple-  
 mented in the Test Model 5 (TM5) reference implementation  
 [8]. In this rate control method, the QP value for each mac-  
 roblock is calculated adaptively based on target bit-allocation  
 and predicted macroblock spatial activity. The Video Model  
 (VM8) used during the development of the MPEG-4 Part 2  
 (Visual) standard uses a more accurate model based on a sec-  
 ond order rate-distortion (RD) relationship [9]. The reference  
 implementation of the AVC standard (Joint Model, JM) uses  
 a rate control method based on a quadratic rate-quantization  
 ( $R-Q$ ) relationship [10], which relies on the assumption that  
 the residual information follows a Laplacian distribution [11].  
 The mean absolute difference (MAD) for the residuals is used to  
 estimate the complexity of basic coding units and corresponding  
 QP. Later on, Kamaci *et al.* [12] showed that a Cauchy distribu-  
 tion is more suitable than Laplacian to represent the residuals,  
 and proposed a frame-level rate control method based on these  
 findings.

Based on the well known quadratic  $R-Q$  model, Choi *et al.*  
 proposed a rate control method [13] which was used in early  
 versions of HEVC reference software (HM) implementation

[14]. However, due to the flexible quadtree partitioning used in HEVC, this  $R$ - $Q$  model is not sufficiently accurate to quantify the relationship between rate and quantization step. Lee and Kim [15] improved this quadratic  $R$ - $Q$  model by proposing a new relationship for inter coding in HEVC based on a mixture of multiple Laplacian distributions. Still targeting the HEVC standard, Lee *et al.* [16] proposed instead a frame-level rate control based on different rate allocation models for the bits spent on texture (e.g. residuals) and non-texture (e.g. motion vectors) data. In this approach, multiple Laplacian distributions are used to model the rate of texture bits, while the rate for non-textured bits is modeled with a linear relationship. All these methods based on the  $R$ - $Q$  model assume that quantization parameter is a crucial factor in determining the bit-rate. However, that condition holds only when other coding parameters (e.g. the coding mode) are fixed. Given the RD optimization operated in HM, along with the flexible quadtree partitioning specified in HEVC, this assumption is not necessarily true, as already pointed out [17].

Another group of rate control methods tries to build a relationship between the rate and percentage of zeros in quantized transform coefficients  $\rho$ . He *et al.* [18] proposed a  $\rho$ -domain model and associated rate control. Based on the estimated RD curves, a rate-shape-smoothing algorithm is proposed to smooth the rate distribution and ensure a consistent picture quality. A quadratic  $\rho$ -domain rate model was proposed by Wang *et al.* [19] and used in a hierarchical bit-allocation scheme for rate control in an HEVC codec. The proposed algorithm uses a linear relationship in  $\rho$ -domain between the bits associated with texture and the number of non-zero transformed coefficients. The number of non-zero transformed coefficients is then modeled as a quadratic function of quantization step. Rate control algorithms based on the  $\rho$ -domain relationship work well in fixed transform size coding schemes. Therefore, in video coding standards such as HEVC which specify variable sizes for transform blocks, the relationship between  $\rho$  and rate is not sufficiently accurate.

The relation between Lagrange multiplier  $\lambda$  and coding rate was firstly analyzed by Li *et al.* [17]. They proposed hyperbolic  $R$ - $\lambda$  model which shows a higher correlation when compared with the aforementioned  $R$ - $Q$  models. The  $R$ - $\lambda$  model was utilized in the state-of-the-art HEVC rate control method, where the bit-budget is allocated using three different levels of granularity. This rate control method was further improved for intra frames [20] using the sum of absolute transformed differences (SATD) as a complexity measure. SATD for original  $8 \times 8$  blocks is calculated and used to allocate the bit-budget. Based on the  $R$ - $\lambda$  model, two approaches for improved bit-allocation have been recently proposed. Li *et al.* [21] proposed a method for largest CU (LCU)-level bit-allocation in HEVC rate control. In this approach, the formulation for optimal bit-allocation is established using the Lagrange multiplier, computed by minimizing the distortion under the given bit-rate constraints. Then, recursive Taylor expansion method is used to obtain the approximate closed-form solution for the optimal LCU-level bit-allocation formulation. Wang and Ngan [22] proposed a method which uses the distortion of collocated coding tree units (CTUs) in the previous frame to establish a linear relationship

between distortion and  $\lambda$ . Based on this distortion model, a different bit-allocation algorithm in  $\lambda$ -domain is applied.

## B. Multi-Pass Rate Control Methods

Although parallel architectures are becoming ubiquitous, not many multi-pass rate control methods have been proposed in the past. In x264 [23], which is one of the most popular AVC software implementations, five different rate control modes are specified. Apart from a two-pass approach, where the target number of bits is predicted based on the frame complexity from full encoding in the first pass, one-pass approaches with fast complexity estimation scheme are also available. In this case, a fast motion estimation (ME) algorithm is performed over a half-resolution version of the frame and SATD of the residuals is used as a complexity measure. After encoding each frame or macroblock, future QPs are updated to compensate for mis-predictions in rate using short- and long-term compensation schemes. In the context of HEVC, Wen *et al.* [24] proposed a rate control method based on  $R$ - $\lambda$  model with pre-encoding. In the pre-encoding step, the video sequence is encoded using only  $16 \times 16$  coding units. Rate for the CUs of size  $64 \times 64$  is then estimated using the rate associated with  $16 \times 16$  CUs.  $R$ - $\lambda$  model parameters, as well as weights for bit-allocation of  $64 \times 64$  coding units, are computed using the data from pre-encoding. They also propose a mechanism for resetting the parameters when a scene change leads the existing model parameters to become obsolete.

Another two-pass rate control method for HEVC was proposed by Wang *et al.* [25] based on the structural similarity (SSIM) index. Coding statistics are collected during the first pass, which is performed using a constant QP. These statistics are then used during the second pass for SOP level bit-allocation. Furthermore, Laplacian-based rate and perceptual distortion models are established to adaptively derive  $\lambda$  and dynamically allocate bits. Rate control at finer granularity levels is performed in a perceptually uniform space. It should be noted that in this case the computational complexity associated with the first pass can be quite high. Deng *et al.* [26] proposed a multi-pass rate control method based on the SATD of the residuals and pre-encoding. Pre-encoding is performed using multiple QP values and a limited set of depths and PU modes to obtain rate, distortion, and SATD data which is then fitted into the SATD-RD model using the least squares method. Estimated data is then used to set the parameters used in rate control. However, this method may be of limited use in practical applications with low latency requirements, due to the computationally expensive pre-encoding step.

## C. Rate Control Methods with Region-Based Bit-Allocation

In addition to general purpose rate control methods, specific region-based rate control methods have been proposed in the context of different video coding standards. Hu *et al.* [27] proposed a region-based rate control method for AVC. In this approach, inter-frame information is utilized to divide each frame into multiple regions based on their RD behavior. Macroblocks with similar characteristics are classified into the same region



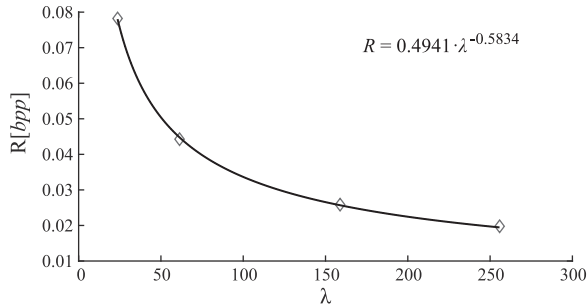


Fig. 1. Fitted  $R$ - $\lambda$  curve for *Manege* test sequence. The sequence was encoded using 4 QP values (27, 31, 35, and 37) and obtained rates are denoted with diamonds.

312 which is treated as a basic unit for the rate control. Recently,  
 313 Meddeb *et al.* [28] proposed a region of interest (ROI) based rate  
 314 control method for HEVC. They divide a frame in tiles which  
 315 correspond to regions with different characteristics. Tiles con-  
 316 taining ROIs are then encoded using different encoder settings  
 317 than non-ROI tiles to achieve better visual quality. The main  
 318 issue for this kind of methods is the ROI detection which is al-  
 319 ways content dependent and when erroneously detected, it can  
 320 lead to poor video quality in regions which attract the attention  
 321 of the observer.

322 A method based on perceptual bit-allocation was proposed by  
 323 Tang *et al.* [29], where a Canny edge detector was used to dis-  
 324 tinguish between randomly-textured, structurally-textured, and  
 325 smooth regions. The method allocates fewer bits to randomly-  
 326 textured regions, given the property of the human visual system  
 327 which is less sensitive to perceptual distortions in textured image  
 328 areas. Another bit-allocation method based on a neurobiologi-  
 329 cal model of visual attention was proposed by Lee *et al.* [30],  
 330 where the model was first used to predict high saliency regions  
 331 in input frames to generate a saliency map. Based on the hu-  
 332 man foveated retina characteristic, top salient locations in the  
 333 saliency map were located and used to generate a guidance map.  
 334 This guidance map was then used to guide the bit allocation pro-  
 335 cess by tuning the QP values. The approach is based on the study  
 336 [31] which showed that a saliency map model can accurately  
 337 predict the human gaze.

#### 338 D. State-of-the-art HEVC Rate Control Method

339 It was shown that there exists a robust relation between the  
 340 rate  $R$  (in bits per pixel) and Lagrange multiplier  $\lambda$  which can  
 341 be expressed with a hyperbolic function [17]:

$$R = a \cdot \lambda^b, \quad (1)$$

342 where  $a$  and  $b$  are parameters related to the video source. An  
 343 example of  $R$ - $\lambda$  relationship is shown in Fig. 1. Due to its im-  
 344 proved accuracy and robustness, the rate control method based  
 345 on the  $R$ - $\lambda$  model defined in (1) has been included in the HM  
 346 reference implementation since version 9.0, and it was there at  
 347 the time of writing (Version 16.7). The algorithm can be divided  
 348 into two parts: bit-allocation, and achievement of target bit-rate  
 349 utilizing the  $R$ - $\lambda$  model. The bit-allocation part is considered at  
 350 three different levels, namely SOP, frame, and basic unit level.

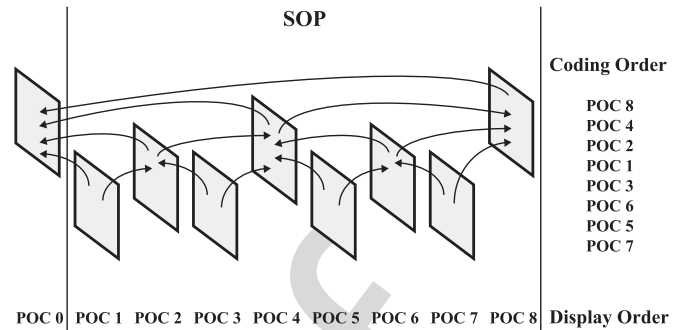


Fig. 2. Random access SOP used in the experiments.

351 Basic unit in this context is represented by  $64 \times 64$  CUs, also  
 352 denoted as CTU in the HEVC standard [4]. When allocating  
 353 bits at a frame-level, each frame is weighted differently depend-  
 354 ing on which hierarchical level in the SOP it belongs to,  
 355 and assuming a random access SOP configuration as used in  
 356 [32]. A picture structure that corresponds to the SOP configu-  
 357 ration used is depicted in Fig. 2, where the picture order count  
 358 (POC) for each picture is shown to highlight the difference be-  
 359 tween display and coding order. The random access SOP also  
 360 defines how the QP changes on a frame basis. More precisely,  
 361 let  $QP_{\text{base}}$ , which is an encoding parameter used to generally  
 362 control the output bit-rate, be the QP value for intra frames,  
 363 then  $QP_{\text{base}} + 1$  will be used for POC 8 frames,  $QP_{\text{base}} + 2$   
 364 for POC 4 frames,  $QP_{\text{base}} + 3$  for POC 2 and POC 6 frames,  
 365 and  $QP_{\text{base}} + 4$  for POC 1, 3, 5 and 7 frames. Throughout this  
 366 paper, when the QP structure is set according to the aforemen-  
 367 tioned values, the encoding will be denoted as variable bit-rate  
 368 (VBR) coding. At basic unit level, the weights to allocate the  
 369 available bit-budget are calculated dynamically using the pre-  
 370 diction error from a collocated basic unit in the previously coded  
 371 frames belonging to the same temporal layer.

372 Once the target rate is determined, it is straightforward to  
 373 determine  $\lambda$  using the inverse of relation (1):

$$\lambda = \alpha \cdot R^\beta, \quad (2)$$

374 where  $\alpha$  and  $\beta$  are model parameters. However, the main prob-  
 375 lem here is how to determine the parameters  $\alpha$  and  $\beta$ , which  
 376 are generally content dependent. Also, in case of random ac-  
 377 cess SOP structure, different temporal layers may have differ-  
 378 ent model parameters, and hence multiple sets of parameters  
 379 have to be used within the sequence. In the existing approach,  
 380 the corresponding  $\alpha$  and  $\beta$  are continuously updated after en-  
 381 coding one basic unit or one frame. Finally, the QP value is  
 382 determined as:

$$QP = c_1 \cdot \ln \lambda + c_2, \quad (3)$$

383 where  $c_1$  and  $c_2$  are set to 4.2005 and 13.7122, respectively.  
 384 Obviously, QP is rounded to the nearest integer value for prac-  
 385 tical use. Finally, to keep the video quality consistent, both  $\lambda$   
 386 and QP should not change significantly with time. Hence,  $\lambda$  and  
 387 QP value range is bounded with respect to the values used in  
 388 previously encoded frame and basic unit.

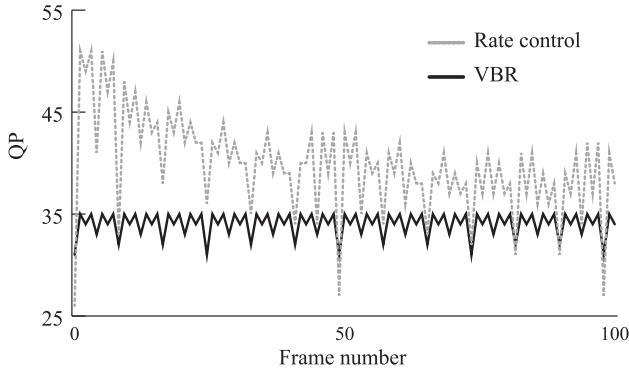


Fig. 3. QP values for the first 100 frames of the *Boxing* test sequence which correspond to the rate obtained with QP value 31 for VBR. QP values used by rate control in HM are denoted with dotted grey line, while QP values associated with the random access SOP are depicted with black.

TABLE I  
TEST MATERIAL DESCRIPTION

| Sequence name    | Fps | Type    | Sequence name | Fps | Type    |
|------------------|-----|---------|---------------|-----|---------|
| ParkAndBuildings | 50  | outdoor | TableCar      | 50  | objects |
| NingyoPompoms    | 50  | objects | TapeBlackRed  | 60  | sport   |
| ShowDrummer1     | 60  | drama   | Hurdles       | 50  | sport   |
| Sedof            | 60  | outdoor | LongJump      | 50  | sport   |
| Petitbato        | 60  | outdoor | Discus        | 50  | sport   |
| Manege           | 60  | outdoor | Somersault    | 50  | sport   |
| ParkDancers      | 50  | outdoor | Boxing        | 50  | sport   |
| CandleSmoke      | 50  | drama   | Netball       | 50  | sport   |

389 Although the rate control method described above shows im-  
 390 proved coding performance compared to previous methods pro-  
 391 posed for HM, it was noticed that it is significantly under per-  
 392 forming at the beginning of the sequence, resulting in degraded  
 393 quality of experience. In particular, very high QP values (up  
 394 to 51 in some cases) were used for frames at the beginning  
 395 of the sequence, as shown in Fig. 3. This is expected, since  
 396 the initial  $\alpha$  and  $\beta$  values for all frame layers are set to prede-  
 397 termined values of 3.2003 and  $-1.3670$ , respectively. That is  
 398 sub-optimal, as  $\lambda$  and corresponding QP value are not calcu-  
 399 lated using the right model parameters. With model parameters  
 400  $\alpha$  and  $\beta$  getting continuously updated, the model will grad-  
 401 ually become more accurate resulting in better visual quality  
 402 with time. However, in applications with frequent or contin-  
 403 uous scene changes, such as broadcasting, this type of behavior  
 404 is highly undesirable, as it results in high quality variations of  
 405 the decoded signal. To overcome this, a two-pass rate control  
 406 method which accurately predicts parameters  $\alpha$  and  $\beta$ , and has  
 407 small latency is proposed in this paper. In the proposed approach,  
 408 a short period at the beginning of the sequence is encoded using  
 409 a reduced set of tools to calculate the initial model parameters  
 410 which are used to improve the encoding performance, espe-  
 411 cially at the beginning of the sequence or after a scene change  
 412 happens.

### 413 III. PROPOSED TWO-PASS RATE CONTROL

414 This section presents the proposed two-pass rate control  
 415 method for compression of UHDTV video content. Besides

describing the proposed method, it is also interesting to analyze  
 the current limitations for the state-of-the-art HEVC rate control  
 method as well as the theoretical performance that can be achieved  
 in case of unlimited computational resources [33], i.e. when the  
 encoder can perform the pre-encoding step testing all possible  
 coding modes to derive the actual bit-rate profile, which is then  
 used in the real encoding step. Throughout the whole section,  
 a fast HEVC encoder implementation based on HM Version 12.0  
 [14] will be considered and denoted as *HM-fast*. For more details  
 about the *HM-fast* codec, the reader is referred to [34]. The  
 test material and experimental conditions are described in the  
 first subsection. Results and findings from the analysis are  
 reported in the second subsection, while the following subsections  
 describe the proposed method.

#### 431 A. Test Material and Coding Conditions

The test set used in this paper is composed of 16 sequences  
 with 8 bits per component, 4:2:0 chroma format,  $3840 \times 2160$   
 spatial resolution, and frame rate of 50 and 60 fps. The names  
 of these sequences, along with the type of content portrayed  
 are listed in Table I. Each sequence is coded with four QP  
 values. They have been determined by visually inspecting the  
 test set compressed with QP ranging from 22 to 45, to deter-  
 mine a good coverage of different visual quality levels: from  
 very good (i.e. coding artifacts unnoticeable) to fairly poor  
 (i.e. coding artifacts visible and annoying). Content denoted  
 as *outdoor* portrays external scenes. Some of these sequences  
 contain water and complex motion (e.g. *PetitBato*, *Sedof* and  
*Manege*) or sharp details and camera panning (e.g. *ParkAnd-*  
*Buildings*), and large area picturing grass (e.g. *ParkAndBuild-*  
*ings* and *ParkDancers*). Content denoted as *drama* corresponds  
 to indoor scenes representative of television drama. Content  
 denoted as *objects* represents indoor scene with moving objects.  
 This content is not fully representative of UHDTV material, but  
 given its spatial and temporal features, is challenging from the  
 compression point of view. Finally, content denoted as *sport*,  
 represents various sports content containing indoor and outdoor  
 sequences.

All the sequences have been encoded according to the Joint  
 Collaborative Team On Video Coding (JCT-VC) common test  
 conditions (CTC) [32] using the selected QP values and the  
 random access main (RA-Main) configuration, as this is repre-  
 sentative of the encoding settings used in broadcasting services.  
 Throughout this paper, compression efficiency and rate inac-  
 curacy are used as performance metrics. For compression effi-  
 ciency, the metric used is the Bjøntegaard delta-rate (BD-rate)  
 computed according to [35] between the anchor data (i.e. the  
 sequences compressed with JCT-VC CTC) and the sequences  
 compressed according to the described experiments. In this con-  
 text, negative BD-rate values will correspond to compression  
 efficiency gains. Given the use of 4:2:0 chroma format, only the  
 BD-rate for the luminance component will be considered. The  
 rate inaccuracy is measured as an absolute percentage deviation  
 from the target rate. Lower value corresponds to higher rate  
 accuracy.

TABLE II  
BD-RATE (BD-R) AND RATE CONTROL INACCURACY (I) FOR THE THREE  
EXPERIMENTS DESCRIBED IN SECTION III-B

| Sequence         | Experiment 1 |            | Experiment 2 |            | Experiment 3 |            |
|------------------|--------------|------------|--------------|------------|--------------|------------|
|                  | BD-R [%]     | I [%]      | BD-R [%]     | I [%]      | BD-R [%]     | I [%]      |
| ParkAndBuildings | 4.2          | 1.3        | 4.7          | 0.0        | 2.3          | 0.0        |
| NingyoPompoms    | 6.5          | 0.0        | 3.5          | 0.0        | 3.5          | 0.0        |
| ShowDrummer1     | 23.4         | 0.0        | 2.2          | 0.0        | 1.2          | 0.0        |
| Sedof            | 3.9          | 0.0        | 5.0          | 0.0        | 5.0          | 0.0        |
| Petitbato        | 8.8          | 0.1        | 2.1          | 0.1        | 1.6          | 0.0        |
| Manege           | 1.4          | 0.0        | 2.6          | 0.0        | 2.0          | 0.0        |
| ParkDancers      | 5.0          | 1.1        | -0.1         | 0.0        | -0.4         | 0.0        |
| CandleSmoke      | 16.2         | 0.0        | 4.2          | 0.0        | 2.3          | 0.0        |
| TableCar         | 8.2          | 1.8        | 2.0          | 0.0        | 1.3          | 0.0        |
| TapeBlackRed     | 13.6         | 0.2        | 2.3          | 0.0        | 0.8          | 0.0        |
| Hurdles          | 8.9          | 0.1        | 2.3          | 0.0        | 2.3          | 0.0        |
| LongJump         | 5.0          | 0.0        | 4.0          | 0.0        | 3.9          | 0.0        |
| Discus           | 4.1          | 0.0        | 3.1          | 0.0        | 3.8          | 0.0        |
| Somersault       | 21.9         | 0.0        | 7.5          | 0.0        | 1.1          | 0.0        |
| Boxing           | 6.5          | 0.0        | 1.5          | 0.0        | 2.3          | 0.0        |
| Netball          | 4.1          | 0.0        | 2.4          | 0.0        | 1.2          | 0.0        |
| <b>Average</b>   | <b>8.8</b>   | <b>0.3</b> | <b>3.1</b>   | <b>0.0</b> | <b>2.1</b>   | <b>0.0</b> |

#### 471 B. Performance Analysis for the State-of-the-art HEVC Rate 472 Control Method

473 This section presents the analysis performed over the state-  
474 of-the-art HEVC rate control method. Three experiments were  
475 conducted. In the first experiment, the coding efficiency of the  
476 existing rate control method in HM is measured in terms of  
477 BD-rate between the coding performance of the *HM-fast* codec  
478 encoded with VBR and *HM-fast* with rate control and using  
479 the bit-rate from VBR as target value. The BD-rate and rate  
480 inaccuracy for the above described experiment are shown in  
481 Table II as *Experiment 1*. As may be noted, the existing rate  
482 control method in HM produces significant coding losses com-  
483 pared with VBR encoding. For instance, BD-rate losses larger  
484 than 20% are reported in some cases. To investigate the possible  
485 source of such high encoding losses, Table III shows the BD-rate  
486 measured on different intra periods for every tested sequence.  
487 As may be noted, the BD-rate penalty is mostly concentrated  
488 at the beginning of the sequence (i.e. in the first intra period).  
489 Average BD-rate penalty for the first intra period is considerably  
490 higher than in the rest of the sequence. This can be explained  
491 by the fact that the existing rate control method in HM uses  
492 predetermined parameter values for  $R-\lambda$  model at the beginning  
493 of the sequence, since it has no prior knowledge of the content  
494 currently being encoded. The rate inaccuracy for all sequences  
495 seems to be sufficiently low.

496 In the second experiment, SOP and frame-level bit-allocation  
497 in the HM rate control method were bypassed, and the bit-  
498 budget was instead derived from the numbers of bits spent on  
499 each frame during VBR encoding. To handle the cases of bit un-  
500 derspending or overspending, a simple rate management scheme  
501 was added to redistribute the differential bits to future frames  
502 based on their weights associated with the SOP used. The frame  
503 weights are determined based on the temporal layer in the SOP

a given frame belongs to and their values are reported in [17].  
This process is repeated after encoding each frame. The aim of  
this experiment is twofold: on the one hand, the bit-allocation as  
designed in the rate control method of HM can be tested and its  
accuracy assessed. On the other hand, also the accuracy of the  
 $R-\lambda$  model can also be thoroughly investigated. The BD-rates  
for the luminance component associated with this experiment  
are shown in Table II and are denoted as *Experiment 2*. It can  
be observed that replacing the existing SOP and frame-level  
bit-allocation, with the frame size obtained from VBR encod-  
ing mode, improves the performance significantly. Moreover,  
the accuracy of achieving the target rate was further improved  
compared to the existing rate control method in HM.

The third experiment aimed to examine the impact of initial-  
izing the model parameters with correct values. As described  
in SubSection II-D, the initial values of parameters  $\alpha$  and  $\beta$  in  
(2) for all temporal layers in the SOP are set to a predetermined  
value in the rate control method of HM. In this experiment, the  
bit-rates and associated  $\lambda$  values, obtained from VBR encoding  
and using four different QP values, were used to fit the  $R-\lambda$   
model from Eq. (2). The fitting is performed differently for each  
SOP temporal layer and for each sequence. The cost minimized  
during the fitting is the sum of absolute differences between the  
QP value predicted by the model and the one used during encod-  
ing. The QP derived by the model is obtained by Eq. (3). The  
reason for minimizing the cost using the QP value is because  
a poor performance of the rate control method was observed  
when minimization was applied to  $\lambda$ . In fact, small differences  
in the  $\lambda$  value may translate into large differences for QP, when  
 $\lambda$  values are small. The  $\alpha$  and  $\beta$  values obtained from the fitting  
were used to initialize the corresponding parameters for frames  
of each temporal layer. As in the previous experiment, SOP  
and frame-level bit-allocation were replaced with the coding  
rate obtained from VBR encoding. The results of this experi-  
ment are shown in Table II as *Experiment 3*. It can be seen that  
the encoding performance of modified rate control method has  
been further improved, with rate inaccuracy achieving almost  
theoretical minimum, i.e. zero.

The results of these experiments show that the existing rate  
control method in HM can be improved by replacing the SOP  
and frame-level bit-allocation with the coding rate associated  
with VBR encoding and initializing the parameters based on  
fitting the actual rate in the  $R-\lambda$  model. However, in practical  
applications, this information is not available prior to encoding  
and in order to obtain it, a full sequence needs to be encoded  
using at least 3 different QP values, resulting in a massive com-  
putational overhead. The proposed rate control method over-  
comes these complexity issues, as explained in the following  
subsections.

#### C. Bit-Rate Profile Analyzer for Pre-Encoding Step

During pre-encoding, a rate control method encodes a given  
video segment (e.g. one SOP or one intra period) and uses the  
coding rate to derive the number of bits spent in each frame.  
Having this information would allow the rate allocation stage  
to distribute the bit-budget accordingly, where the higher the  
rate spent on a frame, the higher the bits allocated to it. This



TABLE III  
BD-RATE (IN PERCENTAGE) PER INTRA PERIOD (IP) DISTRIBUTION. FOR TEST SEQUENCES WITH 50 FPS IP WAS SET TO 48, WHILE FOR 60 FPS SEQUENCES IP WAS SET TO 64. IN CASE THE SEQUENCE HAS LESS THAN 10 IPS, THE VALUES IN CORRESPONDING FIELDS IN THE TABLE ARE MARKED AS N/A

| Sequence         | 1 <sup>st</sup> IP | 2 <sup>nd</sup> IP | 3 <sup>rd</sup> IP | 4 <sup>th</sup> IP | 5 <sup>th</sup> IP | 6 <sup>th</sup> IP | 7 <sup>th</sup> IP | 8 <sup>th</sup> IP | 9 <sup>th</sup> IP | 10 <sup>th</sup> IP |
|------------------|--------------------|--------------------|--------------------|--------------------|--------------------|--------------------|--------------------|--------------------|--------------------|---------------------|
| ParkAndBuildings | 6.9                | 2.7                | 1.7                | 3.5                | 3.8                | 6.3                | 7.0                | 5.2                | 8.4                | 6.6                 |
| NingyoPompoms    | 15.5               | 4.7                | 5.5                | 6.6                | 6.7                | 4.9                | 3.4                | 7.2                | 4.4                | 5.6                 |
| ShowDrummer1     | 29.6               | 9.0                | 4.5                | 38.7               | 29.4               | -4.8               | -0.9               | 23.7               | N/A                | N/A                 |
| Sedof            | 2.9                | 3.4                | 3.0                | 3.5                | 4.4                | 4.9                | 4.4                | 4.4                | 3.9                | N/A                 |
| Petitbato        | 12.1               | 4.8                | 6.2                | 7.3                | 11.0               | 8.3                | 8.9                | 10.8               | 9.7                | N/A                 |
| Manege           | 1.4                | 0.8                | 0.7                | 0.9                | 1.2                | 1.3                | 1.8                | 2.2                | 2.8                | N/A                 |
| ParkDancers      | 4.4                | 6.6                | 8.7                | 6.0                | 0.7                | 3.1                | 14.6               | 8.8                | 4.4                | 1.0                 |
| CandleSmoke      | 32.3               | 6.2                | 19.5               | 7.5                | 32.3               | 7.3                | 22.4               | 5.7                | 5.2                | 5.4                 |
| TableCar         | 5.5                | 15.0               | 24.6               | -1.8               | 9.1                | 0.9                | 7.9                | 1.6                | 2.6                | N/A                 |
| TapeBlackRed     | 29.7               | 4.3                | 7.0                | 7.7                | 7.7                | 6.9                | 7.1                | 5.1                | 5.7                | 3.9                 |
| Hurdles          | 9.2                | 1.7                | 2.9                | 3.1                | 3.3                | 4.0                | 2.8                | 4.2                | 3.8                | 12.4                |
| LongJump         | 5.2                | 3.3                | 5.4                | 3.3                | 6.4                | 3.7                | 11.9               | 4.7                | 9.8                | 2.3                 |
| Discus           | 0.2                | 5.3                | 7.9                | 7.2                | 5.5                | 17.9               | 11.7               | N/A                | N/A                | N/A                 |
| Somersault       | 30.0               | 13.1               | 18.6               | 12.9               | 7.0                | 16.0               | 25.0               | 10.3               | 9.6                | 8.4                 |
| Boxing           | 14.8               | 4.4                | 7.8                | 4.8                | 4.8                | 4.6                | 2.8                | 2.4                | 6.8                | 6.8                 |
| Netball          | 4.3                | 9.6                | 4.3                | 2.1                | 4.0                | 2.0                | 1.2                | 2.7                | 4.8                | 2.7                 |
| <b>Average</b>   | 12.7               | 5.9                | 8.0                | 7.1                | 8.6                | 5.5                | 8.2                | 6.6                | 5.8                | 5.5                 |

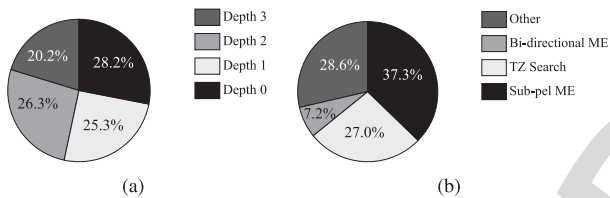


Fig. 4. Percentage of total encoding time spent on testing different coding unit depths (a); and distribution of prediction tasks when the CU depth is equal to zero (b).

560 pre-encoding step is performed in VBR mode and, ideally,  
 561 the encoder should test all possible coding modes that would  
 562 be tested during the actual encoding to obtain a bit-rate profile  
 563 which is as accurate as possible. However, by doing so, the  
 564 amount of complexity involved can be prohibitive, even for ap-  
 565 plications without real time constraints and running on parallel  
 566 computing architectures. One may be also tempted to re-use  
 567 the coding modes derived during pre-encoding for actual com-  
 568 pression to speed up the whole process. However, given that  
 569 those modes were derived for a fixed quantization step, i.e.  
 570 a fixed Lagrange multiplier, they may be sub-optimal when a  
 571 different QP is selected by the rate control method. Therefore,  
 572 the coding modes used during pre-encoding can be only partial-  
 573 ly re-used and the aforementioned claim on computational  
 574 complexity needs to be carefully addressed.

575 In the proposed rate control method, a simplified version  
 576 of *HM-fast* is used. To derive this simplified encoder (*SE*),  
 577 the workload associated with *HM-fast* was profiled to identify  
 578 the most demanding parts in terms of computational complex-  
 579 ity. Fig. 4(a) shows the percentage of encoding time spent on  
 580 testing different CU depths for all sequences belonging to the  
 581 test material. It can be seen that the most encoding time is  
 582 spent while testing CUs at depth 0. Hence, testing of depth  
 583 0 may be considered as the most important among all the  
 584 available depths. Fig. 4(b) shows the distribution of predic-  
 585 tion tasks for CUs at depth 0 for all sequences belonging to

TABLE IV  
PEARSON CORRELATION COEFFICIENT BETWEEN THE CODING RATE FOR  
DIFFERENT SOP TEMPORAL LAYERS SPENT BY *HM-FAST* AND BOTH *SE1*  
AND *SE2* FOR THE ENTIRE TEST SET

| SOP temporal layer | <i>SE1</i> | <i>SE2</i> |
|--------------------|------------|------------|
| Intra              | 0.9841     | 0.9857     |
| 0                  | 0.9578     | 0.9836     |
| 1                  | 0.9559     | 0.9860     |
| 2                  | 0.9670     | 0.9871     |
| 3                  | 0.9604     | 0.9875     |

586 the test set. It can be seen that sub-pel ME is the most time  
 587 consuming inter-prediction module. That is followed by in-  
 588 ter-precision ME and bi-prediction. However, it should be  
 589 noted that some tasks, such as integer precision ME, are critical  
 590 and cannot be removed without greatly affecting the encoding  
 591 process.

592 From this profiling, two configurations for the simplified en-  
 593 coder have been defined and hereafter denoted *SE1* and *SE2*. In  
 594 *SE1*, the size for each CU is set to  $64 \times 64$ , sub-pel (i.e. half-  
 595 and quarter-pel) and bi-directional ME are disabled. In *SE2*,  
 596  $32 \times 32$  CUs are also considered, along with half-pel precision  
 597 ME. Both simplified encoders can significantly reduce the av-  
 598 erage encoder complexity (by almost 75% for the case of *SE1*),  
 599 for considerable drop in coding efficiency. However, as stated  
 600 above, the ultimate goal of the pre-encoding stage is to derive  
 601 the profile on how the coding rate is spent in relative terms, i.e.  
 602 what is the percentage of bits spent on a given frame over the  
 603 total rate used. To measure how accurate the profile derived by  
 604 both *SE1* and *SE2* is, the Pearson correlation coefficient was  
 605 measured on a frame basis between the coding rate spent by  
 606 *HM-fast* and either *SE1* and *SE2*. Table IV shows these corre-  
 607 lation coefficients for different SOP layers. As may be noted,  
 608 even in case of *SE1*, the correlation coefficient is still fairly  
 609 high. This confirms the validity of using the rate obtained from

TABLE V  
PARAMETERS FOR PREDICTING THE RATE FROM SIMPLIFIED ENCODER  
MODEL FOR DIFFERENT SOP TEMPORAL LAYERS

| SOP temporal layer | SE1    |        | SE2    |        |
|--------------------|--------|--------|--------|--------|
|                    | $k$    | $l$    | $k$    | $l$    |
| Intra              | 0.3986 | 1.0576 | 0.4575 | 1.0493 |
| 0                  | 1.1785 | 0.9722 | 0.9462 | 0.9970 |
| 1                  | 0.8126 | 0.9822 | 0.8535 | 0.9951 |
| 2                  | 1.2695 | 0.9421 | 1.4818 | 0.9492 |
| 3                  | 1.8709 | 0.9011 | 1.4378 | 0.9495 |

simplified encoders to estimate the actual rate in unconstrained VBR mode.

Even though good correlation values are obtained for both encoders, the rate spent by either the simplified encoders ( $R_{SE}$ ) is on a different scale with respect to the one spent by *HM-fast* ( $R_{orig}$ ). The reason for this resides in the limited number of coding modes tested by the simplified encoders which results in increased bit-rate compared with encoder operating with the full set of coding tools. To correct the rate values obtained by *SE1* and *SE2*, the following hyperbolic model was used:

$$R_{orig} = k \cdot R_{SE}^l, \quad (4)$$

where  $k$  and  $l$  are model parameters. It should be noted that different parameter values were used for frames at different temporal layers, as shown in Table V. These parameters were derived by performing the least squares fitting on frame data from the test material. This can be formulated as:

$$\arg \min_{k,l} \sum_{i=0}^{N-1} (R_{orig,i} - k \cdot R_{SE,i}^l)^2, \quad (5)$$

where  $N$  is the number of frames from the same SOP temporal layer used for fitting. The output of the pre-encoding stage can be successfully used for SOP and frame-level bit-allocation. However, in order to initialize the parameters for the  $R$ - $\lambda$  model used to derive the QP for each coding block, some additional pre-encoding steps would be required to fit the  $R$ - $\lambda$  curve resulting in increased computational complexity. The next subsection will describe how the proposed rate control method addresses this issue by performing bit-rate profile and model parameters estimation in one pre-encoding step.

#### D. Pre-Encoding with Variable QP Within Frame

Subsection III-B demonstrated that initializing the  $R$ - $\lambda$  model parameters on a per sequence and QP basis led to improved coding performance of the rate control. However, in practical applications, it is not feasible to encode a sequence with different QP values (e.g. 4 values) in order to fit the  $R$ - $\lambda$  model. This section describes the proposed variable QP (VQP) framework designed to reduce the computational complexity associated with the pre-encoding phase in rate control.

The main idea of VQP framework is to encode different CTUs in a frame with different QP values by performing only one, instead of multiple encodings. Accordingly, different CTUs within

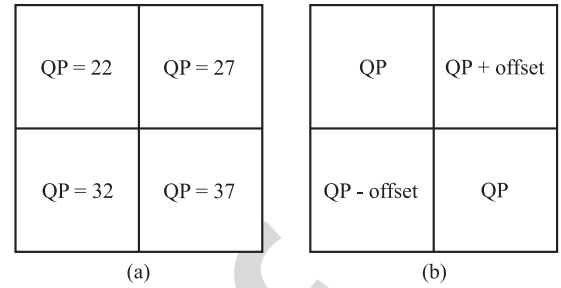


Fig. 5. Variable QP pattern used within a frame for different frame types. Each square represents one CTU. (a) Intra frames. (b) Inter frames.

a frame are encoded with different QP values which are in relation with  $\lambda$  as described in Eq. (3). The rate obtained for those CTUs is collected separately and used to fit the  $R$ - $\lambda$  model defined in Eq. (2) to obtain parameters  $\alpha$  and  $\beta$ .

After the parameters  $\alpha$  and  $\beta$  are available, the actual encoding can be performed. It should be noted that the described VQP is not an additional step performed during pre-encoding, but it is a framework applied during the bit-rate profile analysis described in Section III-C. Therefore, no additional processing is required by the proposed VQP.

Besides using VQP to derive the right  $R$ - $\lambda$  model parameters, it should be noted that it can also be used in the decision on the initial QP value for the first intra frame and the pre-encoding stage. In fact, once the  $R$ - $\lambda$  for the video segment under analysis is available, the target rate value is used to derive the associated  $\lambda$  and QP value using Eqs. (2) and (3), respectively. The QP value derived is then used as the value for the bit-rate profile analysis, as well as for the first intra frame.

The main assumption behind the proposed VQP method, is that CTUs sharing the same QP value are representative of the whole statistics associated with the content. To guarantee this, appropriate sampling of the available CUs should be performed. In this paper, two sampling patterns are defined for intra- and inter-coded frames, as depicted in Fig. 5, where each square represents one CTU. Given that the sampling pattern is regular, each QP value will have associated CTUs coming from different image areas. By considering all tested QP values, the derived points on the  $R$ - $\lambda$  model would allow for a more accurate fitting, rather than if the points were derived from CTUs referring to particular image areas (e.g. texture). For intra-coded frames, the four values in Fig. 5(a) are the same as suggested in [32], while in Fig. 5(b) the offset value is set equal to 2. The reason for using two different patterns in intra and inter frames is because  $R$ - $\lambda$  model for intra frames is used to derive the initial QP, so a wider  $R$ - $\lambda$  curve is needed. Therefore, the four QP values as specified in [32] are used. On the other hand, the VQP pattern for inter frames which is used to derive the  $R$ - $\lambda$  model allows statistics to be collected while not interfering significantly with motion estimation and compensation operated by either *SE1* and *SE2*.

#### E. Workflow of the Proposed Two-Pass Rate Control Algorithm

This section presents the overall workflow associated with the proposed rate control algorithm. As stated above, there are two



---

**Algorithm 1:** Processing for the proposed rate control algorithm.

---

**Require:** Target bit-rate  $\bar{R}$

- 1: Encode the first frame of the video sequence with the VQP pattern in Fig. 5(a)
  - 2: Collect the coding rate  $R_{QP}$  and compute the associated  $\lambda$  for each QP value tested in the VQP pattern
  - 3: Fit the  $R$ - $\lambda$  curve and set the average rate for the first intra picture  $\bar{R}_I$  to  $\bar{R}/F \times 6$ , where  $F$  is the frame rate of a sequence
  - 4: Derive the initial QP,  $QP_{ini}$  using Eqs. (2) and (3), and  $\bar{R}_I$
  - 5: **for all** intra periods in the sequence **do**
  - 6: Encode the current intra period  $IP$  with the simplified encoder ( $SE1$  or  $SE2$ ), encode the intra frame with fixed  $QP_{ini}$  and encode the remaining inter frames with the VQP pattern in Fig. 5(b), where  $QP$  is determined based on SOP temporal layer of a frame
  - 7: Collect the coding rate  $R_I$  for the first intra frame
  - 8: Set  $r_2 = \frac{R_{IP}}{R_I}$  as the ratio between the number of bits obtained for the intra period and intra frame
  - 9: Adjust the rate for the intra frame as  $R_I \leftarrow R_I \times r_2$  and recompute  $QP_{ini}$  using the  $R$ - $\lambda$  curve derived in Step 3
  - 10: For each frame in  $IP$  adjust the allocated bit-budget according to the bit-rate profile derived from the simplified encoder
  - 11: Derive parameters  $\alpha$  and  $\beta$  for the model in Eq. (2) from the data associated with the tested QP values in the VQP pattern in Fig. 5(b)
  - 12: Run actual encoding using the data for rate control derived in the previous steps
  - 13: **end for**
- 

690 main processing steps involved: pre-encoding with the proposed  
 691 VQP method, and encoding with the results gathered from the  
 692 first step. The processing operated by the proposed rate control  
 693 method is summarized in the pseudo code of Algorithm 1.  
 694 Prior to pre-encoding a sequence with VBR mode using VQP  
 695 framework, the initial QP for the intra frame has to be estimated.  
 696 Since only the estimated  $R$ - $\lambda$  curve for the intra frame is avail-  
 697 able prior to performing Step 4 of Algorithm 1, the initial QP  
 698 is estimated using some previously known statistics. However,  
 699 when the ratio between the number of bits spent on intra frame  
 700 and total number of bits spent for all frames in intra period is  
 701 known (i.e. after completing the pre-encoding for a given intra  
 702 period), the initial QP value used during the second-pass CBR  
 703 encoding is recomputed, as described in Step 9.

704 The overall processing for the proposed rate control method  
 705 is also depicted in Fig. 6. The pre-encoding stage introduces a  
 706 delay which can be minimized using multi-threading with one  
 707 thread dedicated to pre-encoding, so that only one intra period  
 708 delay (i.e. approximately 1 second) is introduced. It is worth

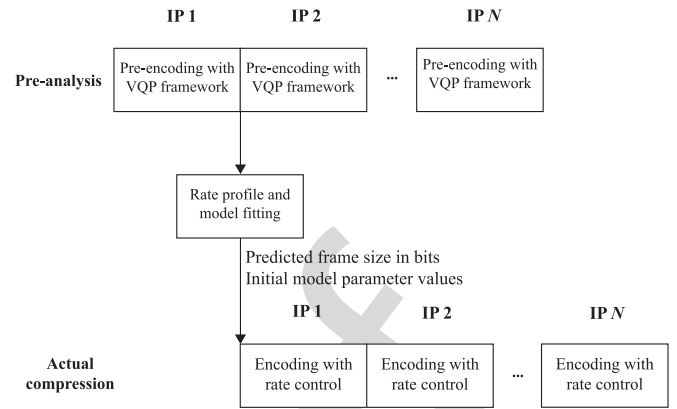


Fig. 6. Block diagram of the proposed approach.

709 pointing out that the delay resulting from pre-encoding of one  
 710 intra period does not imply the usage of a CPB of the same  
 711 size of one intra period. In fact, during the actual encoding  
 712 (Step 12), the size of the CPB can be set according to the  
 713 constraints specified in the selected level and tier.

#### IV. EXPERIMENTAL RESULTS

714 This section presents the performance of the proposed two-  
 715 pass rate control method. The test material, coding configura-  
 716 tion, and performance indicators are the same as described in  
 717 Subsection III-A. All the results presented here will use as refer-  
 718 ence the *HM-fast* codec run in VBR mode. The target rate val-  
 719 ues fed as input to the proposed rate control algorithm will  
 720 be therefore the ones associated with *HM-fast* run in VBR. All  
 721 the tests were run on a Linux cluster of Intel Xeon X3450 with  
 722 2.67 GHz clock frequency and 8 GB of RAM.

723 Table VI shows the experimental results for the proposed  
 724 two-pass rate control method. When compared to the VBR en-  
 725 coding mode, the proposed rate control method achieves an  
 726 average BD-rate coding penalty of 2.9% with 14.8% rate inac-  
 727 curacy. This compares favorably with the state-of-the-art HEVC  
 728 rate control method which provides on average 8.8% BD-rate  
 729 losses with 0.3% rate inaccuracy. It should be noted that even  
 730 though the proposed method provides a lower encoder inac-  
 731 curacy, it still meets the requirements associated with the appli-  
 732 cation scenario considered in the Introduction (i.e. up to 30%  
 733 bit-rate deviation from the target value within a period of 3  
 734 seconds). It is also interesting to analyze the trade-off between  
 735 the two defined simplified encoders used in the pre-encoding  
 736 stage. Therefore, Table VI also shows the BD-rate and rate in-  
 737 accuracy for *SE1* and *SE2*. As expected, *SE2* provides a better  
 738 performance, namely in terms of coding efficiency penalty, with  
 739 respect to *SE1*. When using *SE1* during the pre-encoding and  
 740 replacing the SOP and frame-level bit-allocation with rate pre-  
 741 diction from *SE1*, the proposed rate control method achieves  
 742 4.8% BD-rate losses with 15.2% rate inaccuracy. If initial val-  
 743 ues for  $\alpha$  and  $\beta$  parameters are set based on the model fitting  
 744 using the data obtained from pre-encoding, the proposed en-  
 745 coder achieves on average 3.8% BD-rate losses with 15.2% rate  
 746 inaccuracy. Even better encoding performance can be obtained if  
 747

TABLE VI  
EXPERIMENTAL RESULTS IN TERMS OF BD-RATES (BD-R) AND RATE INACCURACY (I). ALL THE TESTS WERE PERFORMED UNDER THE RA-MAIN CONFIGURATION

| Sequence         | HM rate control |            | SE1 rate control |             | SE2 rate control |             | SE1 rate control with param. init. |             | SE2 rate control with param. init. |             |
|------------------|-----------------|------------|------------------|-------------|------------------|-------------|------------------------------------|-------------|------------------------------------|-------------|
|                  | BD-R [%]        | I [%]      | BD-R [%]         | I [%]       | BD-R [%]         | I [%]       | BD-R [%]                           | I [%]       | BD-R [%]                           | I [%]       |
| ParkAndBuildings | 4.2             | 1.3        | 6.6              | 13.7        | 5.8              | 15.6        | 4.7                                | 13.7        | 4.4                                | 15.6        |
| NingyoPompoms    | 6.5             | 0.0        | 3.9              | 2.3         | 3.3              | 3.1         | 4.9                                | 2.3         | 4.3                                | 3.1         |
| ShowDrummer1     | 23.4            | 0.0        | 10.5             | 36.0        | 9.8              | 33.4        | 9.5                                | 36.0        | 8.8                                | 33.4        |
| Sedof            | 3.9             | 0.0        | 7.8              | 11.2        | 5.8              | 11.6        | 6.3                                | 11.2        | 5.2                                | 11.6        |
| Petitbato        | 8.8             | 0.1        | -1.2             | 13.5        | -1.2             | 14.4        | -1.0                               | 13.5        | -0.7                               | 14.4        |
| Manege           | 1.4             | 0.0        | 10.3             | 7.0         | 5.6              | 7.4         | 8.7                                | 7.0         | 4.2                                | 7.4         |
| ParkDancers      | 5.0             | 1.1        | 1.5              | 5.2         | 2.4              | 5.9         | 1.0                                | 5.2         | 2.1                                | 5.9         |
| CandleSmoke      | 16.2            | 0.0        | 2.4              | 13.5        | 2.5              | 15.3        | 0.9                                | 13.5        | 0.7                                | 15.3        |
| TableCar         | 8.2             | 1.8        | 0.5              | 4.1         | 0.7              | 4.0         | -0.2                               | 4.1         | -0.9                               | 4.0         |
| TapeBlackRed     | 13.6            | 0.2        | 4.0              | 4.8         | 3.3              | 4.4         | 2.8                                | 4.8         | 2.4                                | 4.4         |
| Hurdles          | 8.9             | 0.1        | 5.6              | 20.3        | 2.6              | 19.6        | 5.3                                | 20.3        | 2.4                                | 19.6        |
| LongJump         | 5.0             | 0.0        | 6.0              | 15.2        | 5.4              | 14.5        | 5.1                                | 15.2        | 3.8                                | 14.5        |
| Discus           | 4.1             | 0.0        | 8.2              | 77.1        | 5.2              | 67.6        | 5.8                                | 77.1        | 3.8                                | 67.6        |
| Somersault       | 21.9            | 0.0        | 5.9              | 5.3         | 5.4              | 4.4         | 1.6                                | 5.3         | 1.3                                | 4.4         |
| Boxing           | 6.5             | 0.0        | 2.0              | 4.0         | 1.6              | 7.1         | 2.7                                | 4.0         | 2.5                                | 7.1         |
| Netball          | 4.1             | 0.0        | 2.7              | 9.7         | 2.5              | 8.1         | 2.4                                | 9.7         | 2.2                                | 8.1         |
| <b>Average</b>   | <b>8.8</b>      | <b>0.3</b> | <b>4.8</b>       | <b>15.2</b> | <b>3.8</b>       | <b>14.8</b> | <b>3.8</b>                         | <b>15.2</b> | <b>2.9</b>                         | <b>14.8</b> |

TABLE VII  
EXPERIMENTAL RESULTS IN TERMS OF BD-RATES (BD-R) AND RATE INACCURACY (I) FOR THE MODIFIED RATE ALLOCATION PART. ALL THE TESTS WERE PERFORMED UNDER THE RA-MAIN CONFIGURATION

| Sequence         | HM rate control |            | Modified RC based on SE1 |            | Modified RC based on SE2 |            | SE1 MRC with param. init. |            | SE2 MRC with param. init. |            |
|------------------|-----------------|------------|--------------------------|------------|--------------------------|------------|---------------------------|------------|---------------------------|------------|
|                  | BD-R [%]        | I [%]      | BD-R [%]                 | I [%]      | BD-R [%]                 | I [%]      | BD-R [%]                  | I [%]      | BD-R [%]                  | I [%]      |
| ParkAndBuildings | 4.2             | 1.3        | 6.8                      | 0.3        | 4.6                      | 0.4        | 6.5                       | 0.4        | 5.2                       | 0.4        |
| NingyoPompoms    | 6.5             | 0.0        | 4.1                      | 0.0        | 5.1                      | 0.0        | 3.6                       | 0.0        | 4.5                       | 0.0        |
| ShowDrummer      | 23.4            | 0.0        | 11.4                     | 0.1        | 9.5                      | 0.1        | 11.1                      | 0.1        | 9.0                       | 0.1        |
| Sedof            | 3.9             | 0.0        | 7.7                      | 0.2        | 5.8                      | 0.2        | 6.9                       | 0.2        | 5.0                       | 0.2        |
| Petitbato        | 8.8             | 0.1        | -0.4                     | 0.0        | -1.2                     | 0.1        | 0.0                       | 0.0        | -1.0                      | 0.1        |
| Manege           | 1.4             | 0.0        | 11.0                     | 0.0        | 9.2                      | 0.0        | 7.2                       | 0.0        | 5.3                       | 0.0        |
| ParkDancers      | 5.0             | 1.1        | 2.5                      | 1.3        | 2.4                      | 1.7        | 3.2                       | 1.6        | 3.7                       | 2.3        |
| CandleSmoke      | 16.2            | 0.0        | 8.4                      | 0.5        | 6.9                      | 0.4        | 10.5                      | 0.6        | 7.9                       | 0.5        |
| TableCar         | 8.2             | 1.8        | 1.9                      | 1.1        | -0.1                     | 1.4        | 1.8                       | 1.4        | 1.1                       | 1.5        |
| TapeBlackRed     | 13.6            | 0.2        | 4.7                      | 0.5        | 4.2                      | 0.3        | 4.7                       | 0.6        | 4.5                       | 0.4        |
| Hurdles          | 8.9             | 0.1        | 8.6                      | 0.0        | 9.0                      | 0.0        | 6.0                       | 0.0        | 5.8                       | 0.0        |
| LongJump         | 5.0             | 0.0        | 5.2                      | 0.0        | 3.8                      | 0.0        | 5.9                       | 0.0        | 3.3                       | 0.0        |
| Discus           | 4.1             | 0.0        | 2.1                      | 0.0        | 1.5                      | 0.0        | 2.5                       | 0.0        | 1.0                       | 0.0        |
| Somersault       | 21.9            | 0.0        | 8.8                      | 0.0        | 4.4                      | 0.0        | 9.4                       | 0.0        | 5.2                       | 0.0        |
| Boxing           | 6.5             | 0.0        | 2.7                      | 0.0        | 3.2                      | 0.0        | 2.3                       | 0.0        | 3.8                       | 0.0        |
| Netball          | 4.1             | 0.0        | 2.2                      | 0.0        | 2.1                      | 0.0        | 2.1                       | 0.0        | 2.0                       | 0.0        |
| <b>Average</b>   | <b>8.8</b>      | <b>0.3</b> | <b>5.5</b>               | <b>0.3</b> | <b>4.4</b>               | <b>0.3</b> | <b>5.2</b>                | <b>0.3</b> | <b>4.1</b>                | <b>0.3</b> |

748 *SE2* is used during the pre-encoding. When replacing the SOP  
749 and frame-level bit-allocation with rate prediction from *SE2*,  
750 the proposed rate control method achieves 3.8% BD-rate losses  
751 with 14.8% rate inaccuracy. Finally, when initializing the param-  
752 eters  $\alpha$  and  $\beta$  with data obtained from model using information  
753 from *SE2*, 2.9% BD-rate losses can be achieved for 14.8% rate  
754 inaccuracy.

755 To further improve the accuracy of the proposed algorithm,  
756 an additional experiment was conducted, whereby the frame-  
757 level bit allocation was modified as follows. The weight used  
758 to determine the bit budget for each frame was computed as  
759 the ratio between the coding bits used for that frame and the  
760 total bits spent over the entire intra period by the selected sim-  
761 plified encoder (i.e. *SE1* or *SE2*). The frame weights were then  
762 used to allocate the bits at frame level, assuming equal rate

763 distribution among intra periods in the sequence. Table VII  
764 shows the associated experimental results. It can be seen that  
765 significant accuracy improvements are brought by this new  
766 frame-level bit-allocation. When using *SE1* during the pre-  
767 encoding and replacing the SOP and frame-level bit allocation  
768 with the aforementioned approach, the modified rate control  
769 method achieves 5.5% BD-rate losses with significantly  
770 reduced rate inaccuracy of 0.3%. If the initial values for pa-  
771 rameters  $\alpha$  and  $\beta$  are set based on the model fitting using the  
772 data obtained from pre-encoding, the modified encoder would  
773 achieve an average 4.4% BD-rate losses with 0.3% rate inaccu-  
774 racy. When considering *SE2*, the modified rate control method  
775 achieves on average 5.2% BD-rate losses with reduced rate  
776 inaccuracy of 0.3%. Finally, when also initializing the param-  
777 eters  $\alpha$  and  $\beta$  with data obtained from model using information

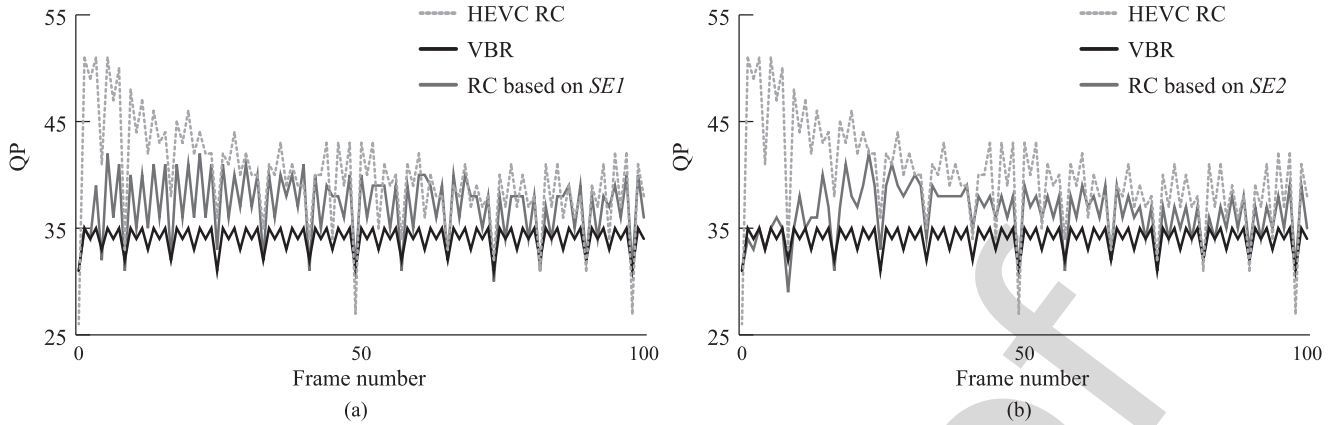


Fig. 7. QP values for the first 100 frames of the *Boxing* test sequence which correspond to the rate obtained with QP value 31 for VBR. QP values for the VBR configuration are depicted with black, QP values used by the state-of-the-art HEVC rate control are denoted with dotted grey line, while QP values used by the proposed rate control method are denoted with solid grey line. (a) Rate control based on *SE1*. (b) Rate control based on *SE2*.

TABLE VIII  
STANDARD DEVIATION OF FRAME PSNRs FOR DIFFERENT ENCODERS

| Sequence             | Standard deviation of frame PSNRs |          |        |        |
|----------------------|-----------------------------------|----------|--------|--------|
|                      | VBR                               | RC in HM | RC-SE1 | RC-SE2 |
| Boxing (QP 23)       | 0.5269                            | 0.7226   | 0.4821 | 0.4891 |
| Boxing (QP 31)       | 0.5538                            | 0.8956   | 0.6318 | 0.5546 |
| ShowDrummer1 (QP 29) | 0.7564                            | 0.8113   | 0.6761 | 0.6513 |
| ShowDrummer1 (QP 36) | 0.4791                            | 0.8181   | 0.6185 | 0.5488 |
| Manege (QP 27)       | 0.5283                            | 0.6940   | 0.4945 | 0.5162 |
| Manege (QP 35)       | 0.5719                            | 0.7814   | 0.7014 | 0.7446 |
| TableCar (QP 24)     | 0.6502                            | 0.6882   | 0.6603 | 0.6594 |
| TableCar (QP 30)     | 0.2705                            | 0.6020   | 0.3151 | 0.3349 |
| Petitbato (QP 25)    | 0.5693                            | 0.7647   | 0.4746 | 0.4711 |
| Petitbato (QP 35)    | 0.6367                            | 0.7676   | 0.6345 | 0.6264 |
| <b>Average</b>       | 0.5543                            | 0.7546   | 0.5689 | 0.5596 |

TABLE IX  
AVERAGE SSIM VALUES FOR THE ANCHOR AND DIFFERENT RATE CONTROL METHODS

| Sequence         | VBR   | HM RC | RC SE1 | RC SE2 | MRC SE1 | MRC SE2 |
|------------------|-------|-------|--------|--------|---------|---------|
| ParkAndBuildings | 0.963 | 0.964 | 0.994  | 0.994  | 0.962   | 0.994   |
| NingyoPompoms    | 0.968 | 0.968 | 0.997  | 0.997  | 0.968   | 0.997   |
| ShowDrummer1     | 0.860 | 0.859 | 0.977  | 0.977  | 0.860   | 0.978   |
| Sedof            | 0.901 | 0.901 | 0.988  | 0.988  | 0.899   | 0.987   |
| Petitbato        | 0.840 | 0.838 | 0.946  | 0.946  | 0.840   | 0.948   |
| Manege           | 0.876 | 0.877 | 0.974  | 0.975  | 0.869   | 0.976   |
| ParkDancers      | 0.866 | 0.868 | 0.965  | 0.965  | 0.867   | 0.965   |
| CandleSmoke      | 0.897 | 0.897 | 0.985  | 0.985  | 0.897   | 0.984   |
| TableCar         | 0.862 | 0.864 | 0.984  | 0.984  | 0.864   | 0.985   |
| TapeBlackRed     | 0.969 | 0.968 | 0.986  | 0.986  | 0.968   | 0.986   |
| Hurdles          | 0.950 | 0.950 | 0.984  | 0.984  | 0.949   | 0.985   |
| LongJump         | 0.951 | 0.950 | 0.989  | 0.990  | 0.950   | 0.989   |
| Discus           | 0.942 | 0.935 | 0.963  | 0.966  | 0.936   | 0.975   |
| Somersault       | 0.950 | 0.950 | 0.977  | 0.977  | 0.950   | 0.977   |
| Boxing           | 0.959 | 0.959 | 0.998  | 0.998  | 0.959   | 0.997   |
| Netball          | 0.952 | 0.952 | 0.984  | 0.984  | 0.951   | 0.983   |
| <b>Average</b>   | 0.919 | 0.919 | 0.981  | 0.981  | 0.918   | 0.982   |

778 from *SE2*, 4.1% BD-rate losses can be achieved for 0.3% rate  
779 inaccuracy.

780 It should be noted that the complexity of the second pass of  
781 the proposed rate control method is not different with respect  
782 to the one of the HM rate control method. As illustrated in  
783 Fig. 6, pre-encoding stage introduces a small latency required  
784 to process the frames related with the first intra period. Using  
785 parallel processing would limit the latency to only initial pre-  
786 encoding for the first intra period.

787 The version of the HM codec used in the experiments does not  
788 implement any scene change detector. However, the behaviour  
789 of the proposed rate control at the beginning of a sequence is  
790 equivalent to what happens after a scene change. In fact, when  
791 a scene change happens, the parameters  $\alpha$  and  $\beta$  of the  $R$ - $\lambda$   
792 model will be reset to their initial values. Moreover, the internal  
793 buffers used to keep track of the QP and  $\lambda$  values for clipping  
794 purposes will be also emptied. This resembles to the same initial  
795 condition at the beginning of the sequence.

796 As described in Subsection II-D, when using the existing  
797 rate control method in HM, QP values at the beginning of the  
798 sequence tend to be much higher than in the VBR case, resulting

799 in degraded Quality of Experience. Fig. 7 shows the comparison  
800 of QP values used at the beginning of the sequence between the  
801 existing and the proposed rate control method. It can be seen  
802 that QP values used by the proposed method are considerably  
803 lower than those used by the existing method, and generally  
804 correlate more with QP values from the VBR encoding mode.

805 Furthermore, since one of the aims of the rate control is to  
806 smooth the visual quality fluctuations in time, visual quality  
807 can also be quantified as the standard deviation of frame-based  
808 PSNR values. Table VIII shows the standard deviation of frame  
809 PSNRs for some of the sequences from the test set. It can be  
810 seen that the standard deviation of PSNR values obtained for  
811 the proposed rate control method based on *SE1* and *SE2* are  
812 significantly lower than the one associated with the HEVC rate  
813 control method. Furthermore, the standard deviation of PSNR  
814 values obtained for the rate control method based on both *SE1*  
815 and *SE2* are very close to the one of unconstrained VBR encod-  
816 ing mode.



817 Finally, the perceptual SSIM metric was computed for the  
 818 anchor and the proposed rate control method with different bit  
 819 allocation schemes. The average SSIM values for test sequences  
 820 are shown in Table IX. It can be seen that almost all versions of  
 821 the proposed rate control algorithm achieve considerably higher  
 822 perceptual quality when compared with the rate control method  
 823 in HM. This verifies the claim that the proposed rate control  
 824 methods also improve perceptual quality.

## 825 V. CONCLUSION

826 UHD TV is expected to deliver an enhanced visual quality  
 827 TV services with the improved Quality of Experience com-  
 828 pared to the existing HDTV services. Apart from higher spatial  
 829 resolution, UHD TV has a potential to deliver wider color  
 830 gamut, high dynamic range and high frame rate. To allow for  
 831 more efficient delivery of such an enormous amount of data,  
 832 the current state-of-the-art HEVC standard has been recently  
 833 developed and standardized. It greatly outperforms the previ-  
 834 ous video coding standards in terms of compression efficiency.  
 835 However, when transmitting a video sequence over a limited  
 836 bandwidth network, visual quality fluctuation with time plays  
 837 a crucial role to provide the high Quality of Experience. Rate  
 838 control in video coding aims to optimize the bit-distribution  
 839 to achieve the highest possible video quality for a given band-  
 840 width constraint. However, in many practical applications with  
 841 frequent scene changes, the existing rate control methods per-  
 842 form sub-optimal, resulting in degraded visual quality at the  
 843 scene beginning. To overcome this issue, a two-pass rate con-  
 844 trol method was proposed in this paper. A simplified encoder  
 845 was used in the pre-encoding stage to obtain the bit-rate profile  
 846 for each intra period. A variable QP framework was designed  
 847 to avoid encoding a sequence multiple times for tuning the  
 848 model parameters. When compared with VBR encoding mode,  
 849 the proposed two-pass rate control method achieves on aver-  
 850 age lower compression losses, 2.9% BD-rate losses compared  
 851 to 8.8% BD-rate losses for the state-of-the-art HEVC rate con-  
 852 trol method. The proposed method also achieves significantly  
 853 higher visual quality. Future research on the proposed method  
 854 may involve integration of the hypothetical reference decoder  
 855 (HRD) model in the rate allocation process with variable buffer  
 856 size, as well as the use of perceptual models to distribute the  
 857 available bit-budget within one picture to further improve the  
 858 perceived video quality.

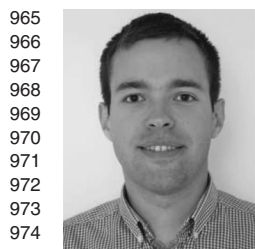
## 859 REFERENCES

- 860 [1] ITU-R, "Parameter values for ultra-high definition television systems  
 861 for production and international programme exchange," ITU-R, Geneva,  
 862 Switzerland, Tech. Rep. BT.2020, Aug. 2012.
- 863 [2] ITU-R, "Parameter values for the HDTV standards for production and  
 864 international programme exchange," ITU-R, Geneva, Switzerland, Tech.  
 865 Rep. BT.709-6, Jun. 2015.
- 866 [3] ETSI, "Digital video broadcasting (DVB); Specification for the use of  
 867 video and audio coding in broadcasting applications based on the MPEG-  
 868 2 transport stream," ETSI, Sophia-Antipolis, France, Tech. Rep. TS 101  
 869 154, Mar. 2015.
- 870 [4] G. Sullivan, J. Ohm, W. Han, and T. Wiegand, "Overview of the high  
 871 efficiency video coding (HEVC) standard," *IEEE Trans. Circuits Syst.*  
 872 *Video Technol.*, vol. 22, no. 12, pp. 1649–1668, Dec. 2012.
- [5] T. Wiegand, G. Sullivan, G. Bjontegaard, and A. Luthra, "Overview of  
 873 the H.264/AVC video coding standard," *IEEE Trans. Circuits Syst. Video*  
 874 *Technol.*, vol. 13, no. 7, pp. 560–576, Jul. 2003. 875
- [6] J. Ohm, G. Sullivan, H. Schwarz, T. K. Tan, and T. Wiegand, "Comparison  
 876 of the coding efficiency of video coding standards—Including high effi-  
 877 ciency video coding (HEVC)," *IEEE Trans. Circuits Syst. Video Technol.*,  
 878 vol. 22, no. 12, pp. 1669–1684, Dec. 2012. 879
- [7] T. K. Tan *et al.*, "Video quality evaluation methodology and verification  
 880 testing of HEVC compression performance," *IEEE Trans. Circuits Syst.*  
 881 *Video Technol.*, vol. 26, no. 1, pp. 76–90, Jan. 2016. 882
- [8] Test Model 5, Feb. 2016. [Online]. Available: <http://www.mpeg.org/MPEG/MSSG/tm5/> 883
- [9] H.-J. Lee, T. Chiang, and Y.-Q. Zhang, "Scalable rate control for MPEG-  
 884 4 video," *IEEE Trans. Circuits Syst. Video Technol.*, vol. 10, no. 6,  
 885 pp. 878–894, Sep. 2000. 886
- [10] K.-P. Lim, G. Sullivan, and T. Wiegand, "Text description of joint model  
 887 reference encoding methods and decoding concealment methods," Joint  
 888 Video Team, Tech. Rep. JVT-N046, Jan. 2005. 889
- [11] T. Chiang and Y.-Q. Zhang, "A new rate control scheme using quadratic  
 890 rate distortion model," *IEEE Trans. Circuits Syst. Video Technol.*, vol. 7,  
 891 no. 1, pp. 246–250, Feb. 1997. 892
- [12] N. Kamaci, Y. Altunbasak, and R. Mersereau, "Frame bit allocation for  
 893 the H.264/AVC video coder via Cauchy-density-based rate and distortion  
 894 models," *IEEE Trans. Circuits Syst. Video Technol.*, vol. 15, no. 8,  
 895 pp. 994–1006, Aug. 2005. 896
- [13] H. Choi, J. Nam, J. Yoo, D. Sim, and I. V. Bajic, "Rate control based on  
 897 unified RQ model for HEVC," Tech. Rep. JCTVC-H0213, Feb. 2012. 898
- [14] HM Reference Software, Jan. 2016. [Online]. Available: <https://hevc.hhi.fraunhofer.de/HM-doc/> 899
- [15] B. Lee and M. Kim, "Modeling rates and distortions based on a mixture  
 900 of Laplacian distributions for inter-predicted residues in quadtree coding  
 901 of HEVC," *IEEE Signal Process. Lett.*, vol. 18, no. 10, pp. 571–574,  
 902 Oct. 2011. 903
- [16] B. Lee, M. Kim, and T. Nguyen, "A frame-level rate control scheme based  
 904 on texture and nontexture rate models for high efficiency video coding,"  
 905 *IEEE Trans. Circuits Syst. Video Technol.*, vol. 24, no. 3, pp. 465–479,  
 906 Mar. 2014. 907
- [17] B. Li, H. Li, L. Li, and J. Zhang, "Lambda domain rate control algorithm  
 908 for high efficiency video coding," *IEEE Trans. Image Process.*, vol. 23,  
 909 no. 9, pp. 3841–3854, Sep. 2014. 910
- [18] Z. He, Y. K. Kim, and S. Mitra, "Low-delay rate control for DCT video  
 911 coding via rho-domain source modeling," *IEEE Trans. Circuits Syst. Video*  
 912 *Technol.*, vol. 11, no. 8, pp. 928–940, Aug. 2001. 913
- [19] S. Wang, S. Ma, S. Wang, D. Zhao, and W. Gao, "Quadratic rho-domain  
 914 based rate control algorithm for HEVC," in *Proc. 2013 IEEE Int. Conf.*  
 915 *Acoust., Speech Signal Process.*, May 2013, pp. 1695–1699. 916
- [20] M. Karczewicz and X. Wang, "Intra frame rate control based on SATD,"  
 917 Tech. Rep. JCTVC-M0257, Apr. 2013. 918
- [21] S. Li, M. Xu, and Z. Wang, "A novel method on optimal bit allocation  
 919 at LCU level for rate control in HEVC," in *Proc. 2015 IEEE Int. Conf.*  
 920 *Multimedia Expo*, Jun. 2015, pp. 1–6. 921
- [22] M. Wang and K. N. Ngan, "Optimal bit allocation in HEVC for real-time  
 922 video communications," in *Proc. 2015 IEEE Int. Conf. Image Process.*,  
 923 Sep. 2015, pp. 2665–2669. 924
- [23] L. Merritt, "x264: A high performance H.264/AVC encoder," Feb. 2016.  
 925 [Online]. Available: [http://akuvian.org/src/x264/overview\\_x264\\_v8\\_5.pdf](http://akuvian.org/src/x264/overview_x264_v8_5.pdf) 926
- [24] J. Wen, M. Fang, M. Tang, and K. Wu, "R-lambda model based improved  
 927 rate control for HEVC with pre-encoding," in *Proc. 2015 Data Compression*  
 928 *Conf.*, Apr. 2015, pp. 53–62. 929
- [25] S. Wang, A. Rehman, K. Zeng, and Z. Wang, "SSIM-inspired two-  
 930 pass rate control for high efficiency video coding," in *Proc. 2015*  
 931 *IEEE 17th Int. Workshop Multimedia Signal Process.*, Oct. 2015,  
 932 pp. 1–5. 933
- [26] L. Deng, F. Pu, S. Hu, and C.-C. J. Kuo, "HEVC encoder optimization  
 934 based on a new RD model and pre-encoding," in *Proc. 2013 Picture Coding*  
 935 *Symp.*, Dec. 2013. 936
- [27] H.-M. Hu, B. Li, W. Lin, W. Li, and M.-T. Sun, "Region-based rate control  
 937 for H.264/AVC for low bit-rate applications," *IEEE Trans. Circuits Syst.*  
 938 *Video Technol.*, vol. 22, no. 11, pp. 1564–1576, Nov. 2012. 939
- [28] M. Meddeb, M. Cagnazzo, and B. Pesquet-Popescu, "ROI-based rate  
 940 control using tiles for an HEVC encoded video stream over a lossy  
 941 network," in *Proc. 2015 IEEE Int. Conf. Image Process.*, Sep. 2015,  
 942 pp. 1389–1393. 943
- 944  
945  
946

- 947 [29] C.-W. Tang, C.-H. Chen, Y.-H. Yu, and C.-J. Tsai, "Visual sensitivity  
948 guided bit allocation for video coding," *IEEE Trans. Multimedia*, vol. 8,  
949 no. 1, pp. 11–18, Feb. 2006.
- 950 [30] Z. Li, S. Qin, and L. Itti, "Visual attention guided bit allocation in video  
951 compression," *Image Vision Comput.*, vol. 29, no. 1, pp. 1–14, Jan. 2011.
- 952 [31] L. Itti, "Automatic foveation for video compression using a neurobiological  
953 model of visual attention," *IEEE Trans. Image Process.*, vol. 13, no. 10,  
954 pp. 1304–1318, Oct. 2004.
- 955 [32] F. Bossen, "Common test conditions and software reference configura-  
956 tions," Tech. Rep. JCTVC-L1100, Oct. 2012.
- 957 [33] I. Zupancic, M. Naccari, M. Mrak, and E. Izquierdo, "Studying rate control  
958 methods for UHD TV delivery using HEVC," in *Proc. 2016 Int. Symp.*  
959 *ELMAR*, 2016, pp. 47–50.
- 960 [34] M. Naccari, A. Gabriellini, M. Mrak, S. Blasi, I. Zupancic, and E.  
961 Izquierdo, "HEVC coding optimisation for ultra high definition television  
962 services," in *Proc. 2015 Picture Coding Symp.*, May 2015, pp. 20–24.
- 963 [35] G. Bjøntegaard, "Improvements of the BD-PSNR model," ITU-T  
964 SG16/Q6, 35th VCEG Meeting, Doc. VCEG-A111, Jul. 2008.



**Marta Mrak** (SM'13) received the Dipl.-Ing. and 998  
M.Sc. degrees in electronics engineering from the 999  
University of Zagreb, Croatia, and the Ph.D. degree 1000  
from the Queen Mary University of London, London, 1001  
U.K. She was a Postdoctoral Researcher with the Uni- 1002  
versity of Surrey, U.K. and the Queen Mary Univer- 1003  
sity of London. She joined the BBC's Research and 1004  
Development Department in 2010, to work on video 1005  
compression research and the H.265/High Efficiency 1006  
Video Coding standardization. She has co-authored 1007  
over 100 papers and co-edited two books. She is an 1008  
elected Member of IEEE Signal Processing Society technical committee on 1009  
Multimedia Signal Processing and IEEE Circuits and Systems Society techni- 1010  
cal committee on Multimedia Systems and Applications. She is also acting as an 1011  
Area Editor of *Signal Processing Image Communication* journal. She has been 1012  
involved in several projects funded by the European Commission and U.K. re- 1013  
search and innovation funds (EPSRC and InnovateUK), and she is coordinating 1014  
Horizon 2020 Innovation Action COGNITUS, while also acting as a Supervisor 1015  
in Marie Curie ITN ProVision. 1016  
1017



**Ivan Zupancic** (S'15) received the B.Sc. degree in 965  
computing and the M.Sc. degree (*cum laude*) in in- 966  
formation and communication technologies from the 967  
Faculty of Electronic Engineering and Computing, 968  
University of Zagreb, Zagreb, Croatia, in 2011 and 969  
2013, respectively. He is currently working toward 970  
the Ph.D. degree with the Multimedia and Vision Re- 971  
search Group, Queen Mary University of London, 972  
London, U.K. His research interests include image 973  
and video coding. 974  
975



**Matteo Naccari** (M'08) received the Laurea degree in 976  
computer engineering and the Ph.D. degree in 977  
electrical engineering and computer science from the 978  
Technical University of Milan, Milan, Italy, in 2005 979  
and 2009, respectively. After earning the Ph.D. degree 980  
he spent more than two years as a Postdoc at the In- 981  
stituto de Telecomunicações, Multimedia Signal Pro- 982  
cessing Group, Lisbon, Portugal. Since September 983  
2011, he joined BBC R&D, London, U.K., as a Senior 984  
Research Engineer working in the video compression 985  
team. His research interests are mainly focused in the 986

video coding area where he works or has worked on video transcoding archi- 987  
tectures, error resilient video coding, automatic quality monitoring in video 988  
content delivery, subjective assessment of video transmitted through noisy chan- 989  
nels, integration of human visual system models in video coding architectures 990  
and encoding techniques to deliver ultra high definition content in broadcasting 991  
applications. He also actively participates to the standardization activities led 992  
by the Joint Collaborative Team On Video Coding where he has served as a 993  
Co-editor for the specification text of the HEVC Range Extensions. He has auth- 994  
ored more than 30 scientific publications for journals, conferences, and book 995  
chapters. 996  
997



**Ebroul Izquierdo** (M'97–SM'03) received the 1018  
M.Sc., C.Eng., and Ph.D. degrees in 1990 and 1993, 1019  
respectively. 1020

He is a Chair of Multimedia and Computer Vi- 1021  
sion and Head of the Multimedia and Vision Group 1022  
in the School of Electronic Engineering and Com- 1023  
puter Science, Queen Mary University of London, 1024  
London, U.K. He holds several patents in the area 1025  
of multimedia signal processing, and has authored or 1026  
co-authored more than 500 technical papers includ- 1027  
ing books and chapters in books. 1028

Prof. Izquierdo is a Fellow of the Institution of Engineering and Technology 1029  
and a Member of the British Machine Vision Association. He is a Chartered 1030  
Engineer, Member of the Visual Signal Processing and Communications Techni- 1031  
cal Committee of the IEEE Circuits and Systems Society and a Member of the 1032  
Multimedia Signal Processing Technical Committee of the IEEE. He is an IEEE 1033  
Circuits and Systems Society Distinguished Lecturer from 2016 to 2017. He 1034  
has been an Associated Editor of the IEEE TRANSACTIONS ON CIRCUITS AND 1035  
SYSTEMS FOR VIDEO TECHNOLOGY (2002–2010) and the IEEE TRANSACTIONS 1036  
ON MULTIMEDIA (2010–2015). He is a Member of the editorial board of several 1037  
other journals in the field. He has been a Member of the Organizing Committee 1038  
of several conferences and workshops in the field of image and video pro- 1039  
cessing including the IEEE International Conference on Image Processing, the 1040  
IEEE International Conference on Acoustics, Speech, and Signal Processing, 1041  
the IEEE International Symposium on Circuits and Systems, the IEEE Visual 1042  
Communications and Image Processing Conference, and the IEEE International 1043  
Conference on Multimedia and Expo. 1044  
1045